

Figure 2. Partially decoupled 270-MHz ^1H - ^{31}P correlation spectrum of the $\text{C}3'\text{H}$ region of $\text{d}(\text{CGCGAATTCGCG})_2$ recorded with scheme B. Both negative and positive peaks are shown. Along the top, a regular resolution-enhanced ^{31}P spectrum is shown; the inset shows a cross section through the $\text{C}3'\text{H}$ cross peak of C1, displaying the antiphase nature of the doublet components. ^{31}P interactions to the $\text{C}4'$ and $\text{C}5'$ protons are "decoupled" in the F_1 dimension. An exponential line narrowing of 1.5 Hz has been used in the F_1 dimension. Assignment of ^{31}P resonances for which the $\text{C}3'\text{H}$ resonances are unresolved was obtained from correlation with $\text{C}4'\text{H}$ (supplementary material).

Table I. $\text{C}3'\text{H}$ - P Coupling Constants (Hz) in $\text{d}(\text{CGCGAATTCGCG})_2$ and Dihedral ϵ Angles (Deg)

$\text{C}3'\text{H}$ nucleotide	scheme A	scheme B	selective ^1H flip	ϵ_{NMR}^g	$\epsilon_{\text{X-ray}}^h$
C1	6.4	6.3	6.4	158	156
G2	3.7 ^a	3.8	3.4	172	179
C3	<i>b</i>	5.5	5.8	161	183
G4	<i>b</i>	4.0	4.0	170	189
A5	2.8	3.3 ^c	2.6 ^d	178	180
A6	<i>b</i>	2.8 ^c	2.3 ^e	181	183
T7	2.7 ^a	3.0 ^c	2.3 ^e	181	181
T8	3.0	3.4 ^c	2.6 ^d	177	187
C9	5.0	5.0	5.1 ^f	163	188
G10	<i>b</i>	3.9	4.2	170	90
C11	5.2	5.2	5.1 ^f	164	173

^a $\text{C}3'\text{H}$ resonance only partly resolved. ^b Coupling could not be determined because of overlap of the $\text{C}3'$ protons. ^c Overestimate of the actual size of the coupling because of partial cancellation of the antiphase doublet components. ^{d-f} Pairs of overlapping ^{31}P resonances. ^g Based on eq 1, using the average coupling, excluding values labeled with *a* and *c* superscripts. ^h From ref 9, averaged over the two non-equivalent strands.

by scheme B. This partial decoupling also gives a significant increase in sensitivity at the expense of the correlations to the $\text{C}4'$ and $\text{C}5'$ protons that are absent in the spectrum. As shown in the inset in Figure 2, the J_{PH} doublet splitting is antiphase. Partial cancellation of such antiphase resonances will occur if the line width is of the same order as the coupling constant. This is the case for the correlations to the $\text{C}3'$ protons of A6 and T7. Therefore, the J_{PH} values measured for these nucleotides represent upper limits for the actual couplings. Considering that the attenuation caused by partial cancellation within the cross peak is nearly identical for A6 and T7, the couplings must be of similar magnitude. These couplings can be measured more accurately with a selective proton-flip experiment,³ the ^{31}P -detected version of scheme A. Couplings measured with the three different techniques are listed in Table I. In this table, the corresponding ϵ angles (obtained by adding 120° to the ϕ angles calculated from

eq 1) are compared with X-ray crystallographic data, showing substantial differences.⁷ A detailed structural analysis of this dodecamer, based on coupling constants and NOE buildup rates, will be presented elsewhere.⁸

The idea of measuring unresolvable couplings by suppressing other splittings, using semiselective pulses, is also applicable to the measurement of homonuclear couplings and can provide information hitherto inaccessible.

Acknowledgment. We thank Gerald Zon for providing us with the sample of $\text{d}(\text{CGCGAATTCGCG})_2$, Bernie Brooks for the X-ray coordinates and dihedral angles, and Rolf Tschudin for making the required spectrometer modifications.

Registry No. $\text{d}(\text{CGCGAATTCGCG})_2$, 77889-82-8.

Supplementary Material Available: Regular ^1H -detected 500-MHz ^1H - ^{31}P correlation spectrum, showing the correlations to $\text{C}3'$, $\text{C}4'$, and $\text{C}5'$ resonances (Figure A), ^{31}P -detected selective proton-flip experiment recorded at 270-MHz ^1H frequency (Figure B), and cross sections through Figure B (Figure C) (3 pages). Ordering information is given on any current masthead page.

(7) For every J_{PH} coupling measured, four possible ϕ values are obtained from eq 1. Three of these four values are discarded because they correspond to torsion angles energetically very unfavorable for B DNA.

(8) Sklenář, V.; Brooks, B.; Zon, G.; Bax, A., manuscript in preparation.

(9) Holbrook, S. R.; Dickerson, R. E.; Kim, S. H. *Acta Crystallogr., Sect. B: Struct. Crystallogr. Cryst. Chem.* **1985**, *41*, 255.

ESR Characterization of Ring-Closed Oxirane Radical Cations via a Novel Alternating Line Width Effect[†]

Ffrancon Williams,*[†] Sheng Dai, Larry D. Snow, and Xue-Zhi Qin

Department of Chemistry
University of Tennessee
Knoxville, Tennessee 37996-1600

Thomas Bally,* Stephan Nitsche, and Edwin Haselbach*

Institut de Chimie Physique
Université de Fribourg Suisse, Perolles
CH-1700 Fribourg, Switzerland

Stephen F. Nelsen* and Mark F. Teasley

Department of Chemistry, University of Wisconsin
Madison, Wisconsin 53706

Received May 26, 1987

There is considerable experimental evidence¹⁻¹² supported by numerous theoretical studies¹³⁻¹⁹ to show that the radical cation

[†] Dedicated to the memory of Dr. Machio Iwasaki who passed away June 17, 1987.

^{*} Author to whom correspondence and requests for reprints should be addressed.

(1) Blair, A. S.; Harrison, A. G. *Can. J. Chem.* **1973**, *51*, 703.

(2) Staley, R. H.; Corderman, R. R.; Foster, M. S.; Beauchamp, J. L. *J. Am. Chem. Soc.* **1974**, *96*, 1260.

(3) Corderman, R. R.; LeBreton, P. R.; Buttrill, S. E.; Williamson, A. D.; Beauchamp, J. L. *J. Chem. Phys.* **1976**, *65*, 4929.

(4) Bouma, W. J.; MacLeod, J. K.; Radom, L. *J. Chem. Soc., Chem. Commun.* **1978**, 724.

(5) Bouma, W. J.; MacLeod, J. K.; Radom, L. *Adv. Mass Spectrom.* **1980**, *8*, 178.

(6) Baumann, B. C.; MacLeod, J. K. *J. Am. Chem. Soc.* **1981**, *103*, 6223.

(7) van Velzen, P. N. T.; van der Hart, W. J. *Chem. Phys. Lett.* **1981**, *83*, 55.

(8) Snow, L. D.; Wang, J. T.; Williams, F. *Chem. Phys. Lett.* **1983**, *100*, 193.

(9) Bally, T.; Nitsche, S.; Haselbach, E. *Helv. Chim. Acta* **1984**, *67*, 86.

(10) Qin, X.-Z.; Snow, L. D.; Williams, F. *J. Am. Chem. Soc.* **1985**, *107*, 3366.

(11) Rideout, J.; Symons, M. C. R.; Wren, B. W. *J. Chem. Soc., Faraday Trans. 1*, **1986**, *82*, 167.

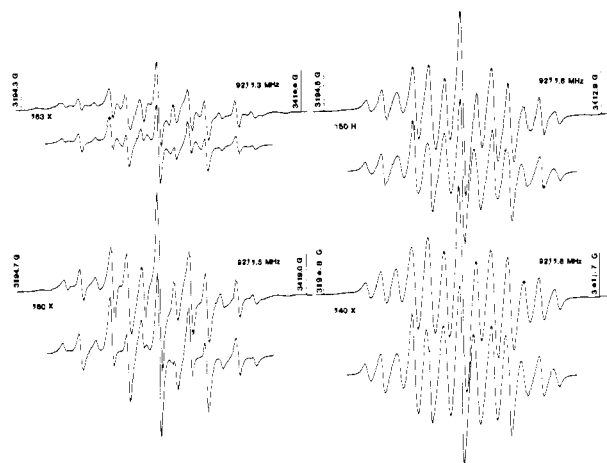
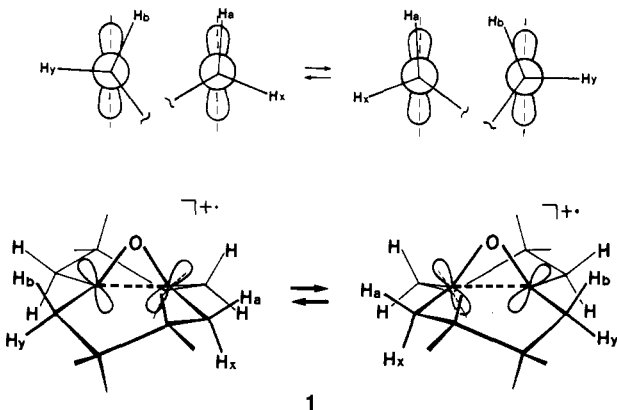


Figure 1. First-derivative ESR spectra of the 9,10-octalin oxide radical cation in CFCl_3 . The simulated spectra shown beneath the experimental spectra were calculated (see text) by using the parameters in Table I, a line width of 2.7 G, and rate constants for ring inversion in **1** of $7.1 \times 10^7 \text{ s}^{-1}$ (163 K), $5.6 \times 10^7 \text{ s}^{-1}$ (160 K), $2.50 \times 10^7 \text{ s}^{-1}$ (150 K), and $1.11 \times 10^7 \text{ s}^{-1}$ (140 K).

formed from oxirane under both gas-phase and solid-state conditions is the planar $\text{C}\cdots\text{C}$ ring-opened oxallyl isomer. In fact, the low barrier to the isomerization^{15,18,19} usually dictates that *only* the ring-opened form can be detected spectroscopically from monocyclic⁸⁻¹² and bicyclic^{11,12} oxiranes at 77 K. These elusive cyclic cations should be accessible, however, in polycyclic oxiranes where steric constraints prevent $\text{C}\cdots\text{C}$ opening of the oxirane ring,⁹ and here we report the first ESR characterization of ring-closed oxirane cations with a one-electron C–C bond.²⁰

The cation of 9,10-octalin oxide [11-oxatricyclo[4.4.1.0^{1,6}]undecane] (**1**) was generated radiolytically²¹ in CFCl_3 at 77 K, and



its ESR spectrum showed a marked temperature dependence below the softening point (165 K) of this matrix, as illustrated in Figure 1 where simulated spectra (vide infra) are also presented. In terms of the most stable half-chair transoid ring conformations²² shown

(12) Williams, F.; Snow, L. D.; Qin, X.-Z.; Bally, T.; Nitsche, S.; Haselbach, E.; Nelsen, S. F.; Teasley, M. F., unpublished results.

(13) Bouma, W. J.; MacLeod, J. K.; Radom, L. *Nouv. J. Chim.* **1978**, *2*, 439.

(14) Bouma, W. J.; MacLeod, J. K.; Radom, L. *J. Am. Chem. Soc.* **1979**, *101*, 5540.

(15) Cimraglia, R.; Miertus, S.; Tomasi, J. *J. Mol. Struct.* **1980**, *62*, 249.

(16) Feller, D.; Davidson, E. R.; Borden, W. T. *J. Am. Chem. Soc.* **1983**, *105*, 3347; **1984**, *106*, 2513.

(17) Bouma, W. J.; Poppinger, D.; Saebo, S.; MacLeod, J. K.; Radom, L. *Chem. Phys. Lett.* **1984**, *104*, 198.

(18) Clark, T. *J. Chem. Soc., Chem. Commun.* **1984**, 666.

(19) Nobes, R. H.; Bouma, W. J.; MacLeod, J. K.; Radom, L. *Chem. Phys. Lett.* **1987**, *135*, 78.

(20) By "ring-closed", we simply mean that rotation about the C–O bonds to the oxallyl species has not occurred, and this description carries no implication about the degree of C–C bonding left in these cyclic radical cations (vide infra).

(21) (a) Shida, T.; Haselbach, E.; Bally, T. *Acc. Chem. Res.* **1984**, *17*, 180. (b) Symons, M. C. R. *Chem. Soc. Rev.* **1984**, *13*, 412.

Table I. ESR and Related Structural Parameters for the Radical Cations of 9,10-Octalin Oxide (**1**) and *syn*-Sesquinorbornene Oxide (**2**) in a CFCl_3 Matrix

radical cation	β - ¹ H hyperfine couplings ^a , G	$\text{H}_\beta\text{C}_\beta\text{C}_\alpha\text{P}_\alpha$ dihedral angles ^b , deg	$\text{H}_\beta\text{C}_\beta\text{C}_\alpha\text{P}_\alpha$ dihedral angles ^c , deg	<i>g</i>
1	35.8 (2H _a) ^d	±4.4 (5.2)	±7.3	2.0050
	25.8 (2H _b) ^d	±32.6 (32.3)	±27.7	
	11.5 (2H _x) ^d	±124.4 (124.4)	±122.6	
	1.5 (2H _y) ^d	±87.4 (78.2)	±89.0	
2	24.2 (4H _β) ^d	±(36.3)		2.0069

^aThe estimated uncertainty in the hyperfine couplings is ±1.5 G for **1** and ±0.5 G for **2**. ^bCalculated from the hyperfine couplings assuming the Heller–McConnell $\cos^2\theta$ equation,^e a planar configuration at C_α, and that the H_aCH_x and H_bCH_y phase angles are both equal to 120°. By using these assumptions and the Powell method^f for a non-linear least-squares error minimization, the proportionality constant in the $\cos^2\theta$ equation^e was also determined to be 36.1 G. The θ values in parentheses were calculated directly from the couplings by using this latter value. ^cAM1-UHF calculated values for the optimized geometry having $d(\text{C}_\alpha, \text{C}_\alpha) = 2.214 \text{ \AA}$ and planar α -carbons. ^dH_a is axial, anti to O, and H_x is equatorial on the same carbon; H_b is axial, syn to O, and H_y is equatorial on the same carbon. ^eHeller, C.; McConnell, H. M. *J. Chem. Phys.* **1960**, *32*, 1535. ^fPowell, M. T. D. *Comput. J.* **1964**, *7*, 303.

in **1**, the rigid-limit spectrum for this carbon-centered C₂ structure at low temperature is expected to show hyperfine coupling to the four completely equivalent pairs of β -hydrogens represented by H_a, H_b, H_x, and H_y. Also, because the dynamic effect of ring flipping brings about the interconversion of H_a and H_b and of H_x and H_y, the spectrum at elevated temperatures should consist of a quintet of quintets. However, this fast-exchange limit is not accessible within the available temperature range, and the key to the spectral interpretation is the recognition of a novel alternating line width effect.

The usual result of slow exchange effects in the above spin system is to selectively broaden the $M_1 = \pm 1$ components in both the primary (2H_a, 2H_b) and secondary (2H_x, 2H_y) quintets.²³ Consequently, the unbroadened lines corresponding to the coalescence spectrum normally constitute a triplet of triplets, the apparent splittings being twice the quintet splittings. However, the coalescence spectrum at 160 K (Figure 1) also shows a doublet of doublets with precisely the same splittings as for the aforesaid triplets. These extra lines are in fact the $M_1 = \pm 1$ components of the primary quintet with a substructure corresponding only to the $M_1 = \pm 1$ components of the secondary quintet. In other words, the spectrum shows an *alternating substructure* of triplets and doublets arising from a change of parity in the line width alternation.

It can easily be shown that this striking effect results from an internal relation between the coupling constants (Table I)²⁴

$$a(2\text{H}_a) - a(2\text{H}_b) = a(2\text{H}_x) - a(2\text{H}_y)$$

which establishes that the position of line components meeting the condition

$$M_1(2\text{H}_a) + M_1(2\text{H}_x) = M_1(2\text{H}_b) + M_1(2\text{H}_y)$$

will remain invariant upon exchange. Our results are illustrated with the aid of the stick plots in the correlation diagram of Figure

(22) This transoid structure was also calculated to be the most stable for the neutral molecule with use of the MM2 program; see, e.g.: Clark, T. A. *Handbook of Computational Chemistry*; J. Wiley and Sons: New York, NY, 1985; Chapter 2, p 112.

(23) Sullivan, P. D.; Bolton, J. R. *Adv. Magn. Reson.* **1970**, *4*, 39.

(24) It should be noted that this relation does not require that H_a and H_x be at one site with H_b and H_y at the other, as found in the present case with $a(2\text{H}_a) > a(2\text{H}_b)$ and $a(2\text{H}_x) > a(2\text{H}_y)$. Retaining these inequalities for definition purposes, the same relationship between the spin states would also apply if H_a and H_y were at one site and H_b and H_x at the other. This latter case may in fact be of more general interest in other kinds of exchange problems since the average coupling at each site now remains the same. In other words, if the average coupling at each site is the same for the two sites undergoing exchange, the internal relation between the coupling constants is prescribed and therefore not fortuitous.

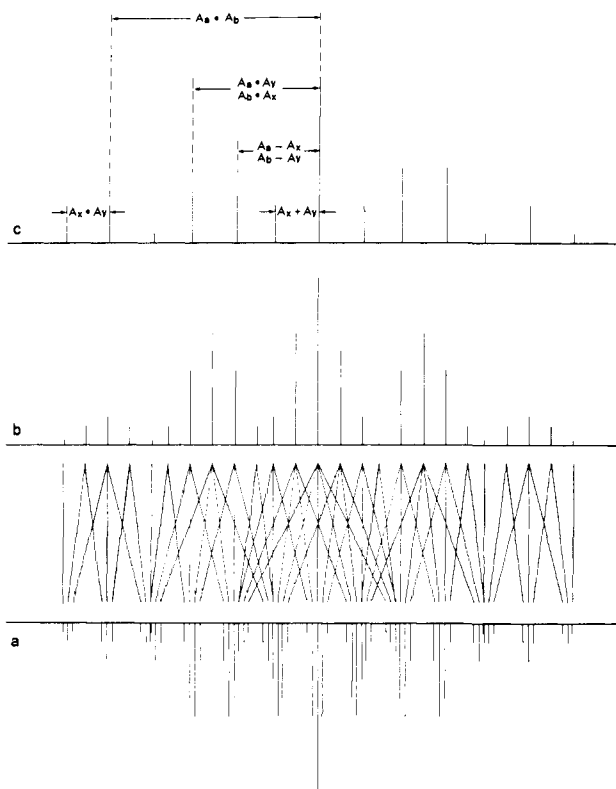
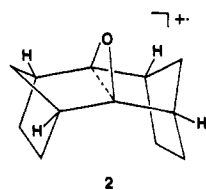


Figure 2. Stick diagram reconstructions of the 9,10-octalin oxide radical cation **1** spectra for (a) slow, (b) fast, and (c) intermediate rates of exchange between $2H_a$ and $2H_b$ and between $2H_x$ and $2H_y$. The intensities of the line components in stick plot b are shown at half scale, and the lines connecting the components in plots a and b show the correlations between nuclear spin states.

2. Thus, the 140-K spectrum in Figure 1 corresponds to the 13 line groups for the rigid-limit spectrum in plot a, while the coalescence spectrum at 160 K fits the reconstruction in plot c of line components whose resonances remain unaltered by exchange (plots a and b). Simulations of the temperature-dependent spectra were made by using the modified Bloch equations for a two-jump model,²³ and the interconversion rate constants used to obtain the fits in Figure 1 obeyed an Arrhenius relation with $A = 5.6 \times 10^{12} \text{ s}^{-1}$ and $E_a = 3.66 \text{ kcal mol}^{-1}$. These parameters are very similar to those reported for ring inversion in the cyclohexyl radical²⁵ and the cyclohexaneseimidone radical anion.²⁶

An obvious corollary is that dynamic effects should be absent in the rigid cation of *syn*-sesquinoxinone oxide (**2**). In



agreement, its ESR spectrum showed no temperature dependence and consisted of a quintet from coupling to the four equivalent bridgehead hydrogens (Table I). Together with the absence of significant *g*-anisotropy for both **1** and **2**, the detection of angular-dependent couplings for hydrogens in β positions with respect to the oxirane ring carbons strongly supports the assignment to carbon-centered rather than oxygen-centered cations. Although high-level *ab initio* MO calculations predict a 2B_1 ground state rather than the analogous carbon-centered 2A_1 state for the ring-closed parent oxirane cation,¹⁹ the change in the state ordering on going to these rigid species is attributable to the effect of

alkylation which is known to destabilize the a_1 relative to the b_1 orbital in methylated oxiranes.²⁷

In fact, AM1 calculations²⁸ confirm that **1** possesses a 2A_1 ground state with transoid C_2 symmetry. Moreover, the calculated dihedral angles for the optimized geometry are in excellent agreement with those deduced from the ESR analysis (Table I). Also, the AM1 calculations reveal that the spin density is largely concentrated in the 2p orbitals of the α -carbons²⁹ which assume a nearly planar configuration with a highly elongated $C_\alpha-C_{\alpha'}$ bond distance of 2.21 Å. Clearly, the C-C bond must be very weak in these intermediate $CC(\sigma)$ species, and their observation is probably only feasible when rotation about the C-O bonds to the more stable oxallyl radical cation^{8-10,16-19} is prohibited, as by the bicyclic ring systems in the present case.

Acknowledgment. Support of this research at the University of Tennessee was provided by the Division of Chemical Sciences, U.S. Department of Energy (report no. DOE/ER/02968-171). The support of the Schweizerischer Nationalfonds (Project No. 2.044-0.86) is also gratefully acknowledged.

Supplementary Material Available: Figure showing the ESR spectrum of the *syn*-sesquinoxinone oxide cation in the $CFCl_3$ matrix (1 page). Ordering information is given on any current masthead page.

(27) (a) McAduff, E. J.; Houk, K. N. *Can. J. Chem.* **1977**, *55*, 318. (b) The photoelectron spectra of tetraalkylated oxiranes indicate that the adiabatic ionization leading to the 2A_1 state may occur at lower energy than that yielding the 2B_1 state.¹²

(28) Dewar M. J. S.; Zoebisch, E. G.; Healy, E. F.; Stewart, J. J. P. *J. Am. Chem. Soc.* **1985**, *107*, 3902.

(29) Both AM1 and INDO calculations on the 2A_1 state of **1** in the optimized geometry indicate that very little spin density (ρ ca. 0.02-0.05) resides in the symmetry-adapted sp orbital on oxygen, as expected because this s-rich orbital is of lower energy and overlaps poorly with the in-plane p orbitals on the α -carbons which carry most of the spin density. Thus the singly occupied orbital can be considered as delocalized between the two α -carbons mainly through space rather than through the C-O bonds or the oxygen lone-pair (*n*) orbital.

Voltammetric Studies of the Interaction of Tris(1,10-phenanthroline)cobalt(III) with DNA

Michael T. Carter and Allen J. Bard*

Department of Chemistry, The University of Texas
Austin, Texas 78712

Received July 7, 1987

We report here how the changes in the cyclic voltammetric (CV) behavior of tris(1,10-phenanthroline)cobalt(III), $Co(phen)_3^{3+}$, in an aqueous medium upon addition of DNA can be used to probe the interaction between these species. Coordination complexes of 1,10-phenanthroline and 4,7-diphenyl-1,10-phenanthroline with Ru(II) and Co(III),^{1,2} and other metal chelates³⁻⁶ that intercalate between the stacked base pairs of native

(1) (a) Barton, J. K.; Danishefsky, A. T.; Goldberg, J. M. *J. Am. Chem. Soc.* **1984**, *106*, 2172. (b) Barton, J. K.; Basile, L. A.; Danishefsky, A. T.; Alexandrescu, A. *Proc. Natl. Acad. Sci. U.S.A.* **1984**, *81*, 1961. (c) Kumar, C. V.; Barton, J. K.; Turro, N. J. *J. Am. Chem. Soc.* **1985**, *107*, 5518. (d) Barton, J. K.; Goldberg, J. M.; Kumar, C. V.; Turro, N. J. *J. Am. Chem. Soc.* **1986**, *108*, 2081. (e) Mei, H.-Y.; Barton, J. K. *J. Am. Chem. Soc.* **1986**, *108*, 7414. (f) Barton, J. K. *J. Biomol. Struct. Dyn.* **1981**, *1*, 621. (g) Goldstein, B. M.; Barton, J. K.; Berman, H. M. *Inorg. Chem.* **1986**, *25*, 842.

(2) (a) Barton, J. K.; Dannenberg, J. J.; Raphael, A. L. *J. Am. Chem. Soc.* **1982**, *104*, 4967. (b) Barton, J. K.; Lolis, E. *J. Am. Chem. Soc.* **1985**, *107*, 708.

(3) Hecht, S. M. *Acc. Chem. Res.* **1986**, *19*, 383.

(4) Subramanian, R.; Meares, C. F. *J. Am. Chem. Soc.* **1986**, *108*, 6427.

(5) Goldstein, S.; Czapski, G. *J. Am. Chem. Soc.* **1986**, *108*, 2244.

(25) Ogawa, S.; Fessenden, R. W. *J. Chem. Phys.* **1964**, *41*, 994.

(26) Russell, G. A.; Underwood, G. R.; Lini, D. C. *J. Am. Chem. Soc.* **1967**, *89*, 6636.